Forsch Ingenieurwes (2023) 87:411–420
https://doi.org/10.1007/s10010-023-00637-y

ORIGINALARBEITEN/ORIGINALS

An investigation into the transferability of dynamic elastomer dampers' properties between different damper sizes using FEM

Tobias Rapp[1] · Georg Jacobs[1] · Joerg Berroth[1] · Stefan Kleinewegen[2]

Received: 31 October 2022 / Accepted: 20 January 2023 / Published online: 20 March 2023

Abstract

Elastomer dampers are used in drive systems to systematically adjust the systems' vibration behavior. Selecting the right damper therefore requires model-based prediction of the system's vibrations. Modelling elastomer dampers in the system context involves a high degree of complexity, since non-linear material effects in elastomers, such as the dependence of material properties on loading speed and history, make it difficult to predict the material behavior. This complexity hinders the model parameters of elastomer dampers to be determined from physical parameters such as material composition and geometric quantities. Instead, abstract models must be used that represent the material behavior phenomenologically and that are parameterized via experimental investigations on each individual damper. The diversity of variants as well as customly produced dampers mean that manufacturers and industrial applicators of elastomer dampers are confronted with disproportionately large numbers of required experiments.

The aim of this work is to reduce the number of required experiments by inferring the behavior of various different elastomer dampers from experiments on a single damper. For this purpose, it is assumed that separating the influence of the damper's geometry and the influence of the material is possible, while the geometries' influence can be predicted by abstracting parts of the phenomenological model via a simple FE model. The method is exemplarily demonstrated by predicting the transmission behavior of two torsional loaded elastomer couplings from experiments on a test specimen. The method is validated by comparing predicted and measured dynamic stiffness of the investigated couplings.

Untersuchung der Übertragbarkeit der dynamischen Eigenschaften von Elastomerdämpfern zwischen verschiedenen Dämpfergrößen mittels FEM

Zusammenfassung

Elastomerdämpfer werden zur gezielten Beeinflussung des Schwingungsverhaltens von Antriebssystemen eingesetzt. Um sicherzustellen, den optimalen Dämpfer auszuwählen, ist die modellbasierte Vorhersage des Systemverhaltens aus Dämpfer und Antrieb erforderlich. Die hierzu notwendige Modellierung des Dämpfers ist jedoch mit einer hohen Komplexität verbunden, da nichtlineare Materialeffekte, wie beispielsweise die Abhängigkeit der Elastomereigenschaften von der Belastungsgeschwindigkeit und -historie, die Vorhersage des Materialverhaltens erschweren. Die Komplexität verhindert, dass die Steifigkeit von Elastomerdämpfern aus physikalischen Größen, wie bspw. der Materialzusammensetzung und der Geometrie, bestimmt werden kann. Stattdessen müssen abstrakte Bauteilmodelle verwendet werden, die das Materialverhalten phänomenologisch abbilden und durch experimentelle Untersuchungen an jedem einzelnen Dämpfer parametriert werden. Die Variantenvielfalt der Dämpfer führt dazu, dass Hersteller und Anwender von Elastomerdämpfern mit einer unverhältnismäßig großen Anzahl an erforderlichen Experimenten konfrontiert sind.

✉ Tobias Rapp
tobias.rapp@imse.rwth-aachen.de

[1] IMSE, RWTH Aachen University, Eilfschornstraße 18, 52062 Aachen, Germany

[2] Flender GmbH, Schlavenhorst 100, 46395 Bocholt, Germany

Ziel dieser Arbeit ist, die Anzahl der erforderlichen Versuche zu reduzieren, indem von Versuchen an einem Dämpfer auf das Verhalten anderer Dämpfer geschlossen wird. Dazu wird der Einfluss der Geometrie vom Einfluss des Materials mittels eines statischen, linearelastischen FE-Modells getrennt. Die Methode wird anhand der Prognose des Übertragungsverhaltens von zwei torsionsbelasteten Elastomerkupplungen aus Experimenten an einem Probekörper demonstriert. Die Übereinstimmung von vorhergesagten und gemessenen dynamischen Steifigkeiten der untersuchten Kupplungen validiert die entwickelte Methode.

1 Introduction

Elastomer dampers are used in almost every drive system to specifically influence the dynamic behaviour of systems [1]. By making use of the dampers' high flexibility, resonances are systematically shifted out of the critical excitation range of the driving machine and damped via the internal damping of the material [2]. In order to shift resonances with pinpoint accuracy, a model-based prediction of the system behaviour based on models of the examined system as well as the damper behaviour is mandatory. While most commonly used machine elements can nowadays be modelled with sufficient accuracy in system simulation, the modelling of elastomer components still remains a challenge [3]. This is due to the fact that the dynamic behaviour of elastomers is characterized by a number of non-linear material effects, some of which change the behaviour of elastomer components depending on the loading situation independently of each other and some are superimposed.

Particularly relevant for system simulation are the material effects a) hyperelasticity, which results in non-linear elastic behaviour (Fig. 1a; [4]), b) viscoelasticity, which results in a time-dependent increase in stiffness with increasing loading rates (Fig. 1b; [5]), and c) Payne effect, which leads to a decrease in stiffness with increasing load amplitude (Fig. 1c; [6]).

In addition to the described material effects, there is another important factor influencing the transmission behaviour of elastomeric components: Due to the low stiffness and the high tolerable strains of elastomers [8], the geometry of elastomer components under load differs considerably from the initial geometry. Depending on the preload, the same external dynamic load accordingly leads to completely different loading conditions in the elastomer. In combination, the geometric and material-dependent nonlinearities can cause changes in the transmission stiffness of elastomer components of over 300% [9]. For a pinpointed system optimization by means of elastomer damping elements, it is therefore mandatory to know the damper's behaviour resulting from the respective load situation.

To determine the dependence of the damper's behaviour on dynamic conditions, a commonly used approach is to conduct experiments under the respective load condition. Here, components are preloaded in several levels and subjected to sinusoidal loads in a dynamic mechanical analysis (DMA) [10]. By varying the load frequency at constant amplitude, conclusions can be drawn regarding viscoelastic behaviour, and by varying the load amplitude at constant frequency, conclusions can be drawn regarding the Payne effect. Since there are no possibilities to differentiate the geometry-dependent non-linear behaviour from the material-dependent non-linear behaviour and thus experimental results cannot be transferred to other components, experiments have to be carried out on each individual to-be-modelled component. These tests are associated with considerable effort, as specialized test rigs with adaptations for each component are required and the complete characterization of a component takes several hours. For manufacturers and applicators of elastomer dampers, which usually exist in several hundred variants, the experimental approach thus represents an unaffordable effort.

Another way of determining the dependence of the damper's behaviour on the dynamic conditions is to perform simulative investigations of the component using the finite element method (FEM). Here, a DMA is performed on an elastomer specimen. Based on the test results, a material model is parameterized to represent the influence of the non-linear material effects on the material behaviour.

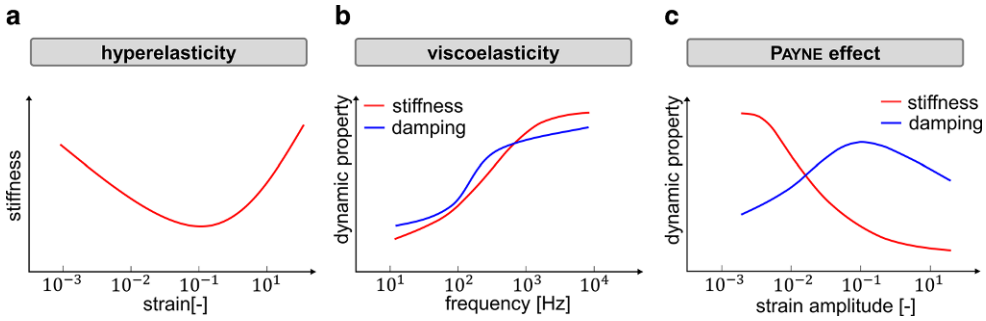

Fig. 1 Overview of relevant material effects in elastomers. (Adapted from [7])

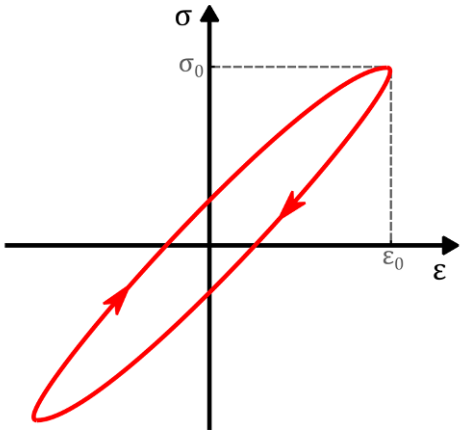

Fig. 2 Hysteresis. (Adapted from Austrell [14])

Material models are available for all relevant material effects [11–13]. The component to be investigated is then geometrically discretized into finite elements to which the material behaviour stored in the material model is assigned. Subsequently, in dynamic simulations, the dynamic conditions to be mapped can be applied to the model, allowing the damper behaviour to be concluded from the simulation results. However, the simulative approach is accompanied by inaccuracies (25%) [3] of the determined damper characteristic values as well as considerable numerical and modelling efforts. Even if a material model is already available, the dynamic elastomer simulation in the FEM imposes demanding requirements on the model quality due to the very large deformations of the material, which results in the effort of the simulation generally being greater than the effort of experimental investigations. The FEM is therefore also not a suitable method for the dynamic characterization of elastomer components.

Overall, today no method exists to determine characteristic values of elastomer components that requires neither experimental investigations of each component nor dynamic FE simulations. As a consequence, the dependence of dynamic elastomer properties on the load condition is usually neglected in system simulation, which leads to a low validity of the models. Accordingly, this work aims to develop a method to efficiently determine the dynamic characteristics of elastomeric components (i.e. stiffness) and the dependence on the load condition for varying frequency, amplitude and preload. The method is based on performing reference measurements on an elastomer component (specimen or size variant of the same material) and transferring the measured properties to to-be-modelled components. For this purpose, static and therefor efficient FE simulations of the tested and the to-be-modelled component are carried out deploying arbitrary linear material parameters. Based on these simulations the geometrically non-linear behaviour of the components is investigated to determine how the to-be-modelled component is to be loaded so that the material in both components is subjected to the same load condition. Based on the assumption of resulting same material properties, loads measured on the tested component are scaled to the to-be-modelled component in the identified load condition, also using static linear FE simulation.

2 Related work

As described in Chap. 2, the behaviour of elastomer components is significantly influenced by non-linear material effects. A prerequisite for being able to correctly represent this influence in simulation is to quantify the effects on the basis of descriptive variables. The most frequently used descriptive variable for characterizing elastomers is the stiffness. Determining the stiffness can be achieved based on the hysteresis (cf. Figure 2). The hysteresis is the plot of load versus deformation obtained in a DMA in the reference state of harmonic sinusoidal deformation. According to Austrell [14], the dynamic stiffness c can be determined from the quotient of the load amplitude F_0 and deformation amplitude s_0 (cf. Equation 1).

$$c = \frac{\sigma_0}{\varepsilon_0} \tag{1}$$

Accordingly, the stiffness at precisely defined load conditions can be understood as an expression of the material behaviour. If the material effects described in Chap. 2 are to be characterized, only the stiffness at different frequencies, amplitudes and prestresses must be determined.

3 Methods

The method developed in this work pursues the goal of efficiently determining the dependence of the dynamic stiffness of any elastomer component on the loading condition by means of tests on a specimen of the same material but

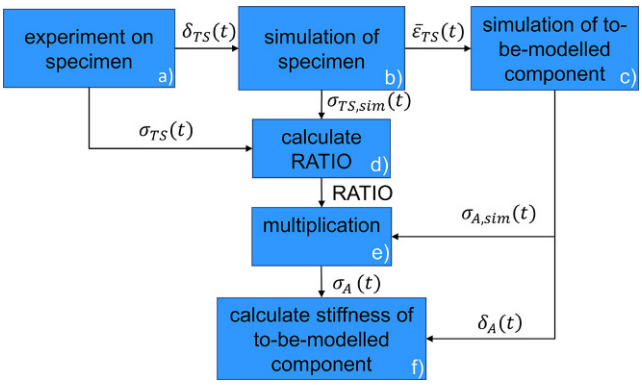

Fig. 3 Workflow of the developed method

different geometry. The method comprises the procedure outlined in Fig. 3. First, deformations $\delta_{TS}(t)$ are experimentally imposed on the test specimen (TS) while loads $\sigma_{TS}(t)$ are measured (Fig. 3a), which allow for the dynamic stiffness of the specimen to be determined as a function of the nonlinear material behaviour described in Chap. 2. The influence of the non-linear material behaviour on the specimen's behaviour is then determined using FE simulations. For this purpose, the test specimen is modelled in FEM, with the elastomer being replaced by a linear material of arbitrary stiffness. By simulatively applying the deformation of the tests (Fig. 3b), a simulated external load $\sigma_{TS,sim}(t)$ is determined which is independent of any non-linear material behaviour. The ratio of simulated and measured external load (referred to as RATIO in the following; Fig. 3d) changes as a result of and is an expression of the non-linear material behaviour. In order to transfer this RATIO to other components, it is assumed that the material behaviour in elastomer components can be approximated by an average material behaviour and that this average material behaviour is proportional to the course of the average strain in this component. Accordingly, the RATIO of two components is identical if both components experience the same course of their average strain. Based on the fact that most elastomers exhibit isotropic behaviour [15], it is additionally assumed that the deformed geometry of elastomer components for the same external deformation is independent of the material properties. It follows that the average strain can be determined on the basis of FE simulations with arbitrary material parameters. Accordingly, the FE simulation of the specimen (Fig. 3b) is used to determine the course of the average strain in the specimen $\overline{\varepsilon}_{TS}(t)$ when loaded by the external strain applied in the test. Subsequently, a FE simulation of the to-be-modelled component A (Fig. 3c) is used to determine which external deformation $\delta_A(t)$ is to be applied to that to-be-modelled component in order to produce the same course of the average strain and thus the same RATIO. By simulatively determining the external load

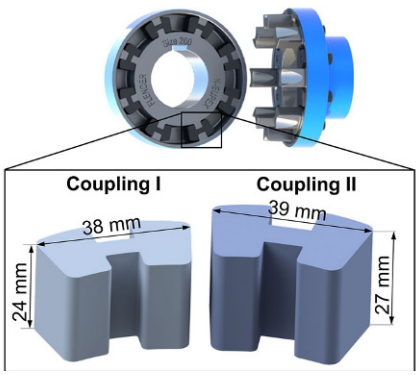

Fig. 4 Rendering of one of the investigated couplings and comparison of the elastomer elements of both couplings

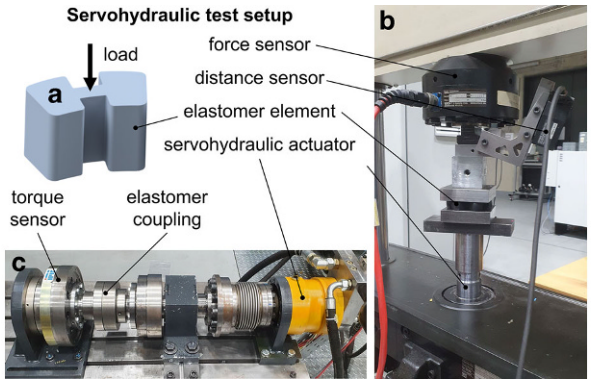

Fig. 5 **a** Tested elastomer element; **b** Setup for experiments on the elastomer elements; **c** Setup for experiments on the elastomer couplings

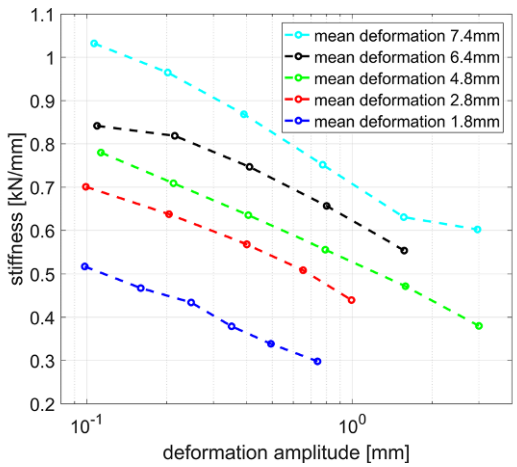

Fig. 6 Translational stiffness vs. deformation amplitude for the elastomer element

of the to-be-modelled component $\sigma_{A,sim}(t)$ and multiplying it with the RATIO, the actual external load $\sigma_A(t)$ (Fig. 3e) and thus also the stiffness of the to-be-modelled component (Fig. 3f) can be calculated according to Chap. 3.

The following chapters describe how the mentioned interrelations can be applied to real elastomer components. Chapter 4.1 describes both, the tests performed on the specimen as well as the tests performed on the to-be-modelled component to validate the method. Chapter 4.2 includes a description of the FE calculations and Chap. 4.3 describes the implementation of the developed method.

3.1 Experimental setup & design of experiment

In order to demonstrate its applicability, the developed method is applied to two different elastomer claw couplings. Both couplings are composed of two main components made of steel, each of which can be connected to a shaft via a feather key connection (cf. Figure 4). One of the components holds the elastomer elements, while the other side comprises claws, which after mounting, are

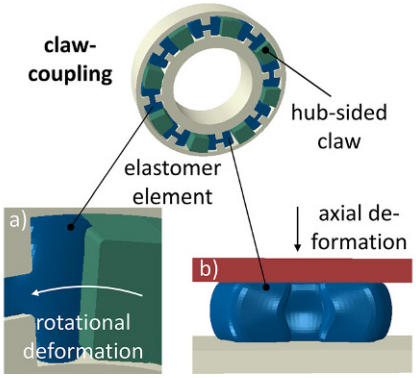

Fig. 7 Deformed FE Models of: a) The elastomer coupling I and b) The elastomer element

each positioned between the elastomer elements. Through the connection of the claws and the elements, torque can be transmitted between the two coupling components and by that between the connected shafts. The two couplings investigated in this work belong to the same coupling variant and differ in size. The smaller coupling is referred to as Coupling I and differs from the other coupling (Coupling II) in diameter as well as in shape of the elastomer elements. The elastomer elements of both couplings are made of the same carbon-black filled natural rubber (NR) with a shore A hardness of 60 and a (quasi-) static shear modulus of 0.59 N/mm^2.

To obtain information on the material behaviour, one elastomer element of coupling I was investigated in experiments and therefor fulfils the role of the specimen, introduced in Chap. 4. Figure 5a visualizes the load direction on the elastomer element studied in the experimental setup shown in Fig. 5b. In the experiment, the element is loaded in compression by means of a servo-hydraulic actuator (MTS: Load Unit 318) in a load direction rotated by 90° compared to its load direction in the coupling. The reaction forces are measured by a strain-gauge based force sensor ($\pm 3N$), while the distance is evaluated by a laser sensor ($\pm$0,007mm). Data acquisition is performed with a measurement amplifier attaining a sampling rate of 1024 Hz.

For validation purposes, further tests were carried out on the two claw couplings. The deployed test setup, in which the couplings can be loaded with a torsional angle, is shown in Fig. 5c. In this setup, measurement data is recorded with a maximum sampling rate of 1024 Hz with an uncertainty of $\pm 5\,Nm$ for torque and $\pm 0.004°$ for angle.

The deployed test procedure is based on the DMA described in Chap. 2, with each test consisting of a sinusoidal deformation with a frequency of 5 Hz at constant test parameters (amplitude and mean deformation). Between each test, the test parameters were varied. The result of each test consists in a time-dependent vector for load, which is a force for the elastomer elements ($F_{TS,i}(t)$ for test i) and a torque for the couplings, and a time-dependent vector for the deformation, which is a displacement for the elastomer elements ($s_{TS,i}(t)$ for test i) and an angle for the couplings. From the test results, the stiffness can be determined as a function of the test parameters following Eq. 1. The result of the experiments on the elastomer element deploying the test setup shown in Fig. 5b is exemplarily shown in Fig. 6.

3.2 Static linear FE-simulation

In order to apply the method developed in this work, it is necessary to perform static linear FE simulations of both the investigated specimen (i.e. elastomer element) and the to-be-modelled component (i.e. elastomer coupling). For these simulations, the investigated components were modelled in a FEM software (Fig. 7) and loaded in the same deformation direction, that was applied in the experiment. The simulations were performed using the software Abaqus (Simulia), assigning a linear stiffness of $1\,N/mm^2$ to the elastomer, while metallic components were represented as rigid bodies. The use of the static simulation approach ensures the ease of use of the method, since here the modelling and computational effort are minimal.

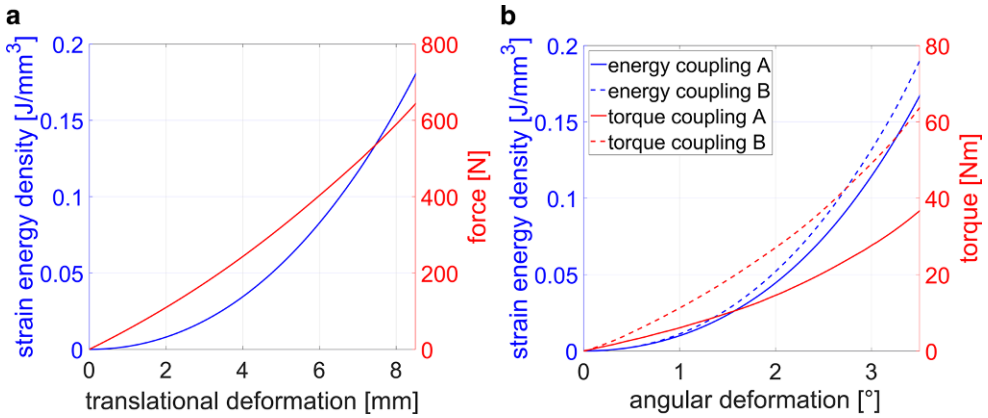

Fig. 8 Simulated strain energy density and external loads as a function of the deformation for the test specimen (**a**) and the elastomer couplings I and II (**b**)

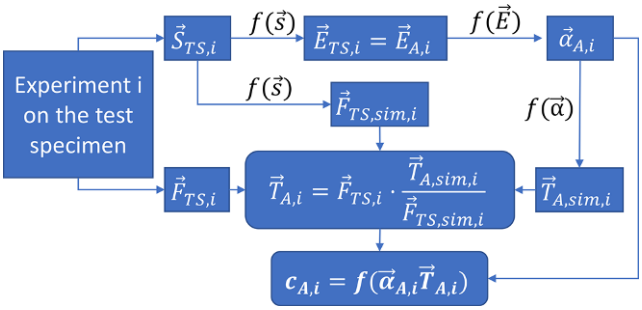

Fig. 9 Flowchart of the developed method

According to Chap. 4, the average strain and the external load are to be derived from the simulation results. While the external load can be easily read out in commercial simulation programs, the determination of the average strain is not possible directly. For this reason, a correlation resulting from the linearity of the calculation is used: The directly output strain energy $E_{st,i}$ can be converted into the distortion energy density E_i via the (constant) volume V of the elastomer component via Eq. 2.

$$E_i = \frac{E_{st,i}}{V} \tag{2}$$

By using the fact that the sought-after average strain $\bar{\varepsilon}_i$ is linked to the strain energy density via the (constant) proportionality factor stiffness c (Eq. 3), the interrelation in Eq. 4 can be found.

$$E_i = \frac{1}{2} \cdot c \cdot \bar{\varepsilon}_i{}^2 \tag{3}$$

$$\bar{\varepsilon}_i \sim \frac{E_{st,i}}{V} \tag{4}$$

Accordingly, the simulation result for the test specimen (elastomer element) consists of the reaction force $F_{TS,\mathrm{sim}} = f(s)$ and the distortion energy density $E_{TS} = f(s)$ as a function of the translational deformation s and for the to-be modelled component (coupling I & II) in reaction torque $T_{A,\mathrm{sim}} = f(\alpha)$ and the distortion energy density $E_A = f(\alpha)$ as a function of the deformation angle α (cf. Figure 8). Since the simulation results are available as a vector, it is possible to invert the functions using linear interpolation. Thus, not only distortion energy densities can be calculated from deformations, but also deformations from distortion energy densities.

3.3 Implementation of the developed method

The developed method was implemented in a Matlab function and follows the procedure visualized in Fig. 9, which is the application of the method presented in Fig. 3. The starting points of the procedure are the experiments on the specimen (cf. Chapter 4.1), which provide a vector for the measured translational deformation $\vec{S}_{TS,i}$ and the reaction force $\vec{F}_{TS,i}$ for each test i. Following Chap. 4.2, the course of the strain energy density in the specimen $\vec{E}_{TS,i}$ as well as the course of the simulated reaction force $\vec{F}_{TS,\mathrm{sim},i}$ are determined from the translational deformation via linear interpolation of the functions in Fig. 8. According to Chap. 4, the material behaviour of two components of the same material is the same if both components exhibit the same course of the average strain, which is proportional to the strain energy density. Thus, by equalling the strain energy density of the to-be-modelled component $\vec{E}_{A,i}$ and the strain energy density of the specimen $\vec{E}_{TS,i}$, the deformation angle of the to-be-modelled component $\vec{\alpha}_{A,i}$ and

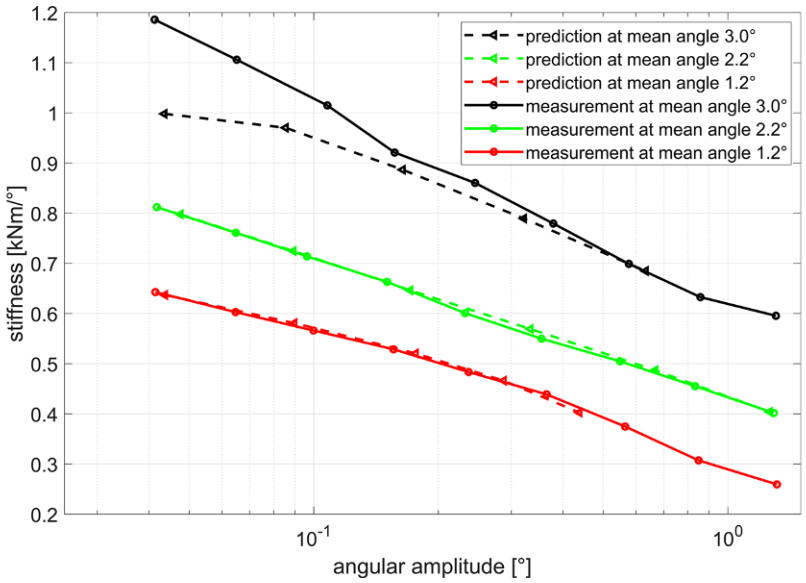

Fig. 10 Stiffness vs angular amplitude at 3 different levels of mean deformation angles for coupling I

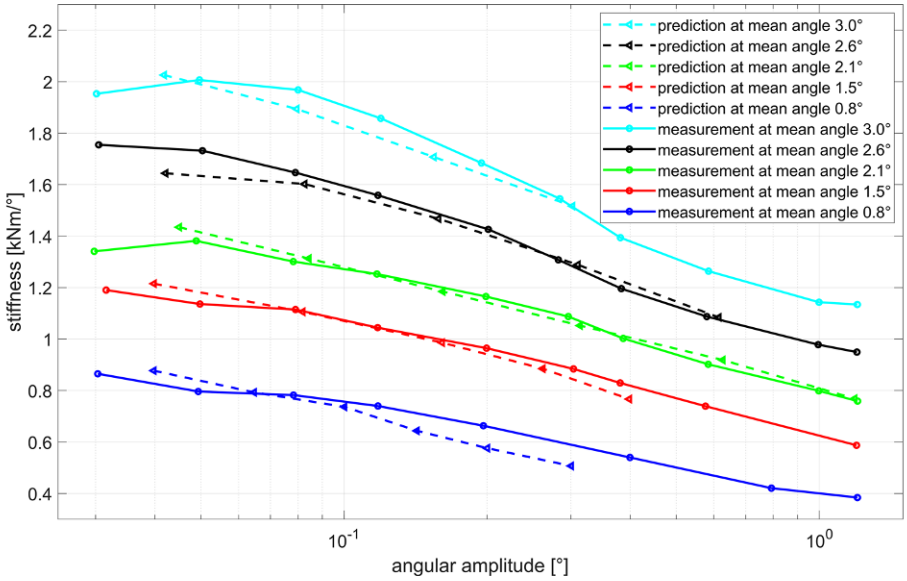

Fig. 11 Stiffness vs angular amplitude at 5 different levels of mean deformation angles for coupling II

the simulated external load $\vec{T}_{A,\mathrm{sim},i}$ are obtained via linear interpolation of the functions in Fig. 8.

According to Chap. 4 the equality of strain energy densities ensures the equality of the RATIO, which describes the ratio of actual external load to simulated loads, leading to Eq. 5 and by that to the external load of the to-be-modelled component $\vec{T}_{A,i}$.

$$\frac{\vec{T}_{A,i}}{\vec{T}_{A,\mathrm{sim},i}} = RATIO = \frac{\vec{F}_{TS,i}}{\vec{F}_{TS,\mathrm{sim},i}} \rightarrow \vec{T}_{A,i} = \vec{F}_{TS,i} \cdot \frac{\vec{T}_{A,\mathrm{sim},i}}{\vec{F}_{TS,\mathrm{sim},i}} \tag{5}$$

Based on the deformation $\vec{\alpha}_{A,i}$ and the external load component $\vec{T}_{A,i}$, the sought-after stiffness $c_{A,i}$ of the to-be-modelled component is determined following Chap. 3.

4 Results

The application of the developed method to predict the stiffnesses of the investigated elastomer couplings and a subsequent comparison with measured coupling stiffnesses (described in Chap. 4.1) is intended to validate the method. The only inputs to the method are the result of the experiments described in Chap. 4.3, in which an elastomer element of coupling I was loaded in axial direction.

In Fig. 10, the predicted stiffnesses of coupling I are compared to measured stiffnesses at various operating conditions. It can be seen that both, the method and measurement, give similar stiffness curves. As the angular amplitude increases, the stiffness decreases for the same mean angle. Larger mean angles result in larger stiffnesses in all cases. Also quantitatively, good agreement between prediction and measurement is observed. For mean angles of 1.2° and 2.2°, the deviations are always smaller than 2%. At the largest mean angle of 3.0°, deviations of up to 20% can be observed in the range of small amplitudes.

In order to show that the good agreement between prediction and measurement is not only due to the fact that one of the predicted coupling's elements was investigated as a test specimen, but that the method actually allows the prediction of the stiffness of completely different components, the method was also applied to the geometrically deviating coupling II. Figure 11 shows the comparison of predicted stiffness for this coupling with measured stiffness in five different amplitude sweeps, each with different mean deformation angles. It can be seen clearly that prediction and measurement agree well in all areas. Coupling II, similar to coupling I, shows the trend of decreasing stiffness with increasing angular amplitudes and increasing stiffness with increasing mean deformation angles. This trend is correctly predicted by the method, even with higher absolute accuracy than for coupling I. Although the measured stiffness changes by a factor greater than 4 in the studied parameter space, the prediction error is always lower than 10%.

5 Discussion

In Chap. 5, stiffnesses determined from two different elastomer couplings were compared with measured stiffnesses based on tests on a specimen and static FE simulations. Good agreement was found between the predicted stiffnesses and the measured stiffnesses, with average deviations of less than 5%. The hypothesis that the material behaviour of elastomers can be described on the basis of an average material behaviour as a function of the mean strain in the

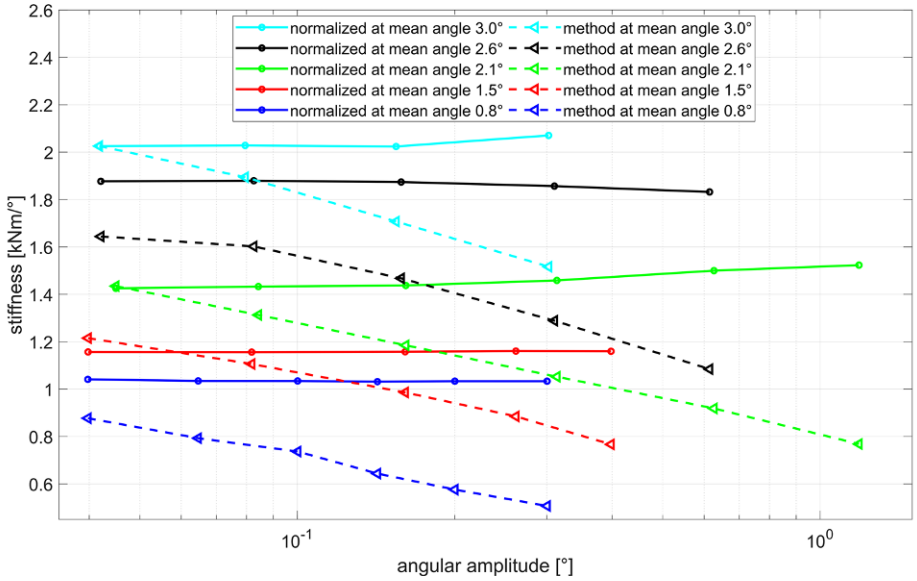

Fig. 12 Comparison of normalized stiffnesses calculated from linear FE simulation over angular amplitude vs. stiffness predicted by the developed method over angular amplitude

component (cf. Chapter 4) could thus be confirmed for the investigated elastomer components.

However, the mere comparison of predicted and measured stiffnesses is not sufficient to show that the method actually does the intended and transfers the influence of non-linear material behaviour from tests on the specimen to the to-be-modelled component. It is also conceivable that the non-linearity of the material has hardly any influence on the component behaviour. In the developed method, the non-linear component behaviour is decomposed in geometry-related and material-related non-linear behaviour, in which the material-related behaviour is represented by the RATIO (Chap. 4). If there was hardly any influence of the material-related non-linearity, the RATIO was a constant factor and the stiffness predicted by the method was proportional to the stiffness calculated solely by FE simulations (from angle $\vec{\alpha}_{A,i}$ and reaction moment $\vec{T}_{A,\mathrm{sim},i}$, with reference to Chap. 4.2), which deploy linear material properties. Figure 12 compares both stiffnesses. The FE stiffnesses were normalized to the point of maximum stiffness of the full model, to exclude an influence of the constant RATIO in case of linear material behaviour. It can clearly be seen that the FE stiffnesses, which only represent the geometry-related non-linearity, exhibit a completely different course than the stiffnesses calculated using the developed method. While the stiffnesses of the developed method decrease with increasing amplitude, the stiffnesses of the FE model are mainly constant for each level of mean angle. Also, the maximum stiffnesses at the smallest amplitude of each level of mean angles don't match between the developed method and the FE model. These differences can only occur due to material-related non-linearities of the elastomer. Since the prediction of the developed method matches the measured coupling behaviour well, the developed model actually does the intended and transfers the influence of non-linear material behaviour from tests on the specimen to the to-be-modelled component.

The comparison of the predicted stiffnesses using the developed method with the measured stiffnesses showed an overall good agreement with average deviations < 5%. However, for coupling I, a significantly larger deviation of up to 20% is observed in the range of large mean angles of 3° and small amplitudes (cf. Figure 10). The course of the stiffnesses measured in the coupling experiments indicates that the deviation is due to inaccuracies in that coupling measurement. The first three stiffness data points at angular amplitudes between 0.04° and 0.15° show a different course than the data points at larger angular amplitudes. A further investigation of the coupling measurements confirms this assumption: In the three critical measurements, superimposed oscillations of higher order can be seen in the course of the measured torques, which lead to an increase in the evaluated torques used to calculate the stiffness. These oscillations are presumably due to resonances in the test setup, which only occur at the three critical operating points, as the coupling stiffness only at this operating point causes the resonance to be critical. Nevertheless, since the stiffness changes by a factor of 4 between the operating point of the smallest mean angle with the largest amplitude and the operating point of the largest mean angle with the smallest amplitude, even the observed deviations of up to 20% are still comparatively small. The method was therefore validated despite the deviations of up to 20% at three data points.

The greatest advantage of the developed method is that the transmission behaviour of any elastomer component can be predicted without having to carry out time-consuming tests on the to-be-modelled component or equally time-

consuming dynamic simulations. While a model for static simulation, as used in this work, can be built in 30 min and simulated in another 5 min, the effort required to model an elastomer component for dynamic simulation is several days, requires specialized knowledge, and involves many hours of computation. The method thus has the potential to significantly reduce the effort required to model elastomers.

A clear disadvantage of the method is that the load conditions to be represented still have to be investigated experimentally. It is possible to draw conclusions from one component to another. However, the initial components must be tested in all relevant operating conditions. Thus, a large part of the effort for the tests in the setup time, is eliminated, but the effort for the test execution cannot be reduced. Nevertheless, great potential is apparent in the further development of the method: If the method can be combined with a sufficiently accurate model of the test specimen, the behaviour of elastomer components of arbitrary geometry under arbitrary loading conditions could be predicted with minimum effort.

Furthermore, it is necessary to investigate where the limits of the developed method lie. The experiments carried out show that the transmission behaviour of the two investigated couplings can be derived from experiments on a test specimen. However, both in the tests on the specimen and in the tests on the couplings, the elastomer is loaded mainly in compression. Whether the method allows conclusions to be drawn on components loaded in tensile or shear direction is not conclusively researched yet.

6 Conclusions

A method for determining the stiffness of elastomer components based on tests on components of arbitrary geometry and the same material has been developed. The method involves performing static finite-element calculations deploying arbitrary linear material properties to identify loading conditions in which the non-linear material behaviour of the to-be-modelled components equals the material behaviour of the tested component. It was demonstrated that the same material behaviour occurs if the course of the mean strain in both components is identical. Thus, it is possible by means of the newly developed method, to predict the transmission behaviour of any elastomer component without carrying out time-consuming tests on the component or equally time-consuming dynamic simulations.

The functionality of the method was demonstrated by application to two different elastomer couplings. Based on tests on a single elastomer element, which was extracted from one of the couplings, the dependence of the coupling stiffness on the influencing variables deformation angle amplitude and mean deformation angle was predicted with mean deviations of less than 5%, while the coupling stiffness varied by more than 400%. The developed method thus represents an accurate and simultaneously time-saving alternative to currently used methods for determining the transmission behaviour of elastomer components.

However, further research is required to firstly validate the range of validity of the method, which so far has only been applied to elastomers loaded in compression, and secondly to avoid the persistently high experimental effort to acquire the necessary test data on the test specimen. The developed approach should be extended with a model of the experimentally investigated specimen in order to model the transmission behaviour of components of the same material of arbitrary geometry and under arbitrary loading conditions without any additional tests.

Funding Open Access funding enabled and organized by Projekt DEAL.

Conflict of interest T. Rapp, G. Jacobs, J. Berroth and S. Kleinewegen declare that they have no competing interests.

References

1. Gao P, Liu H, Xiang C, Yan P, Mahmoud T (2021) A new magnetorheological elastomer torsional vibration absorber: structural design and performance test. Mech Sci 12(1):321–332. https://doi.org/10.5194/ms-12-321-2021
2. Ramos ACR, Santos RB, Melo CAP, Perez IC (2016) Vibroacoustic transfer function study in the design of vehicle suspensions. SAE Technical Paper 2016-36-0242. https://doi.org/10.4271/2016-36-0242
3. Bergström MBJS (1998) Constitutive modeling of the large strain time-dependent behavior of elastomers. Mech Phys Solids 46(5):931
4. Ogden RW, Saccomandi G, Sgura I (2004) Fitting hyperelastic models to experimental data. Comput Mech 34(6):484–502. https://doi.org/10.1007/s00466-004-0593-y
5. Findley WN, Lai JS, Onaran K (1976) Creep and relaxation of nonlinear viscoelastic materials: with an introd. to linear viscoelasticity, 18th edn. Elsevier, Amsterdam (http://www.123library.org/book_details/?id=100782)
6. Payne AR (1962) The dynamic properties of carbon black-loaded natural rubber vulcanizates. Part I. J Appl Polym Sci 6(19):57–63. https://doi.org/10.1002/app.1962.070061906
7. Olsson AK (2007) Finite element procedures in modelling the dynamic properties of rubber. Lund University, Lund

8. Shintake J, Piskarev Y, Jeong SH, Floreano D (2018) Ultrastretchable strain sensors using carbon black-filled elastomer composites and comparison of capacitive versus resistive sensors. Adv Mater Technol 3(3):1700284. https://doi.org/10.1002/admt.201700284
9. Rapp T, Jacobs G, Berroth J, Guenther J (2022) Determining dynamic properties of elastomer-dampers by means of impact testing. Exp Mech. https://doi.org/10.1007/s11340-022-00832-y
10. Ramorino G, Vetturi D, Cambiaghi D, Pegoretti A, Ricco T (2003) Developments in dynamic testing of rubber compounds: assessment of non-linear effects. Polym Test 22(6):681–687. https://doi.org/10.1016/S0142-9418(02)00176-9
11. Yeoh OH (1993) Some forms of the strain energy function for rubber. Rubber Chem Technol 66(5):754–771. https://doi.org/10.5254/1.3538343
12. Bergstrom J (1998) Constitutive modeling of the large strain time-dependent behavior of elastomers. J Mech Phys Solids 46(5):931–954. https://doi.org/10.1016/S0022-5096(97)00075-6
13. Feng X, Xu P, Zhang Y (2018) Filled rubber isolator's constitutive model and application to vehicle multi-body system simulation: a literature review. SAE Int J Veh Dyn Stab NVH 2(2):101–120. https://doi.org/10.4271/10-02-02-0007
14. Austrell P.E., "Modeling of elasticity and damping for filled elastomers," Dissertation, Division of StructuralMechanics, Lund University, Lund, 1997.
15. Li Y, Iwakura Y, Nakayama K, Shimizu H (2007) Highly anisotropic properties of thermoplastic elastomer composites with aligned hierarchical structures. Compos Sci Technol 67(13):2886–2891. https://doi.org/10.1016/j.compscitech.2007.04.007